Journal of Robotics and Control (JRC)
Volume 6, Issue 3, 2025
ISSN: 2715-5072, DOI: 10.18196/jrc.v6i3.26818

Nonlinear Control of Engine Speed Regulation Using Grey Wolf Optimizer for Enhanced System Stability and Performance

Serdar Ekinci [1], Davut Izci [2*], Mostafa Jabari [3], Alfian Ma'arif [4]
[1, 2] Department of Computer Engineering, Istanbul Gedik University, 34876, Istanbul, Turkey
[2] Department of Electrical and Electronics Engineering, Bursa Uludag University, 16059, Bursa, Turkey
[2] Applied Science Research Center, Applied Science Private University, Amman, 11931, Jordan
[3] Faculty of Electrical Engineering, Sahand University of Technology, Tabriz, Iran
[4] Department of Electrical Engineering, Universitas Ahmad Dahlan, Yogyakarta, Indonesia
Email: [1] ekinciser@yahoo.com, [2] davutizci@gmail.com, [3] m_jabari97@sut.ac.ir, [4] alfianmaarif@ee.uad.ac.id
*Corresponding Author

***Abstract*—Accurate control of internal combustion engine speed, especially under variable load conditions, has always been a significant challenge in the automotive industry. Classical PID controllers often fail to effectively compensate for nonlinearities and environmental disturbances in spark ignition (SI) engines. To address this issue, we propose a method based on tuning PIDF controller parameters using the grey wolf optimizer (GWO) to enhance system stability and performance. This approach aims to reduce steady-state error, settling time, and overshoot. A mathematical model of the engine speed control system is developed, and the GWO algorithm is applied to optimize the PIDF gains. The performance of the GWO-based controller is then compared to other metaheuristic methods such as particle swarm optimization (PSO), differential evolution (DE), and cuckoo search (CS) algorithms through simulation. Simulation results demonstrate that the proposed GWO-based approach outperforms the alternatives by achieving better error reduction, improved stability, enhanced disturbance rejection, and faster response times.**

***Keywords*—Engine Speed Control; Grey Wolf Optimizer; PIDF Controller Design; Stability Enhancement; Optimization.**

I. INTRODUCTION

Regulating the speed of internal combustion engines, particularly spark ignition (SI) engines, remains a critical challenge due to their nonlinear dynamics and sensitivity to load variations and external disturbances. In this study, we propose a novel control strategy in which the parameters of a proportional-integral-derivative with filter (PIDF) controller are optimally tuned using the grey wolf optimizer (GWO) algorithm to improve system stability, dynamic response, and steady-state accuracy.

PID controllers are among the most widely used control strategies in engine speed regulation due to their simple structure and ease of implementation [1][2]. However, their performance heavily relies on accurate gain tuning, which becomes particularly challenging in nonlinear systems such as SI engines [3]. Traditional PID controllers often fail to maintain stability and precision under varying conditions, prompting researchers to propose improved versions like filtered PID (PID-F) controllers [4] and advanced designs such as feedforward-compensated PI [5][6] or fractional-order controllers [7], aiming to enhance robustness and dynamic response.

To address these limitations, a wide range of metaheuristic optimization algorithms have been employed for automatic PID tuning in engine control applications [8]. Among the most notable are particle swarm optimization (PSO) [9], differential evolution (DE) [10], cuckoo search (CS) [11], ant colony optimization (ACO) and the recently proposed GWO [12][13]. These algorithms, inspired by natural and evolutionary processes, have demonstrated remarkable capabilities in handling nonlinear, multi-modal, and time-varying dynamics, making them well-suited for engine speed regulation tasks.

In recent years, numerous studies have explored the application of metaheuristic optimization algorithms for enhancing the performance of control systems, particularly in nonlinear and dynamic environments [14][15]. The GWO has emerged as a promising algorithm due to its strong convergence characteristics, ability to avoid local minima, and reduced computational complexity [16][17]. For instance, Nayak, et al. [18] employed GWO for parameter estimation of photovoltaic (PV) models and demonstrated its superiority over traditional algorithms like PSO in terms of accuracy and convergence speed under varying environmental conditions. Similarly, Mohanty, et al. [19] applied the GWO algorithm for maximum power point tracking (MPPT) in PV systems under partial shading conditions. Their results showed that GWO outperformed conventional techniques such as perturb and observe (P&O) and improved PSO (IPSO), particularly in achieving smooth and accurate tracking of global peaks. In the context of power systems, Guha, et al. [20] investigated the use of GWO in load frequency control of multi-area interconnected power networks. They optimized the gains of PI and PID controllers using an integral time absolute error (ITAE) performance index, and reported that GWO delivered better dynamic performance compared to other evolutionary algorithms such as comprehensive learning PSO and DE. In robotics and automation, Rahmani, et al. [21] proposed a novel sliding mode control approach enhanced with an extended GWO (EGWO) to manage a 2-DOF robot manipulator. Their hybrid

controller combined the benefits of both SMC and PD control while leveraging EGWO for parameter tuning. Their comparative simulations confirmed that the NSMC-EGWO method achieved better tracking accuracy and robustness than conventional SMC and PDSMC strategies. Additionally, in the field of cyber-security, Chatterjee, et al. [22] introduced a multi-stage intrusion detection framework that used GWO for feature selection in network traffic data. This framework combined stacked auto encoders and decision tree classifiers, and achieved detection accuracies of over 99% on benchmark datasets, highlighting the algorithm's adaptability across different domains. Al-Tashi, et al. [23] conducted an extensive review on GWO-based feature selection methods for classification tasks, demonstrating the algorithm's effectiveness in reducing dimensionality and identifying relevant features with high accuracy. Although their study focused on machine learning applications, the demonstrated robustness and adaptability of GWO make it a promising candidate for tuning control parameters in complex systems such as engine speed regulation. Geleta, et al. [24] employed GWO to determine the optimal sizing of a hybrid wind and solar renewable energy system, aiming to minimize the total annual cost. Their research indicates that GWO can effectively handle complex optimization problems in energy systems, suggesting its potential applicability in other engineering domains, including engine speed control.

Czarnigowski [25] proposed a model-based control algorithm employing a neural network observer to estimate additional engine loads. Their approach dynamically adjusted the spark advance angle to counteract external disturbances, demonstrating superior performance compared to traditional PID and adaptive controllers, especially under abrupt load variations. Similarly, Yildiz, et al. [26] introduced an adaptive posicast controller (APC) tailored for idle speed regulation in SI engines with time-delay characteristics. Their method, integrated with an existing spark-based controller and implemented via electronic throttle control, significantly reduced the calibration effort and improved disturbance rejection. Duarte, et al. [27] analyzed the feasibility of applying model predictive control (MPC) strategies to control auto-ignition in SI engines. The proposed control strategies focus on maintaining the temperature at the ignition point below the auto-ignition threshold of the fuel–air mixture, thereby preventing knocking and enhancing engine performance. Zhu, et al. [28] presented a nonlinear model predictive control (NMPC) strategy complemented by a disturbance observer. This approach effectively addresses the nonlinearities and external disturbances inherent in SI engines with EGR systems, enhancing engine performance and reducing emissions. Wang, et al. [29] introduced a fuzzy logic-based ignition timing control system for SI engines. This system utilizes a pressure sensor to determine the optimal timing, aiming to enhance engine performance and efficiency. The implementation of this fuzzy control strategy demonstrated improvements in engine operation, highlighting the potential of intelligent control techniques in automotive applications. Sahu and Srivastava [30] investigates the performance of an idle speed controller employing various cylinder airflow calculation methodologies. The research demonstrates that accurate modeling of cylinder airflow significantly improves the controller's ability to maintain stable engine idle speeds under varying operating conditions.

While the aforementioned studies have significantly advanced the state of engine control through adaptive, predictive, and intelligent techniques, few have explored the integration of bio-inspired metaheuristic optimization methods particularly GWO for precise PIDF tuning in spark-ignition engine speed control. This gap highlights the need for further investigation into such approaches, which motivates the present study. The main contribution of this study lies in the implementation of a GWO-based PIDF tuning method for SI engine speed control and its comprehensive comparison with other popular optimization techniques. The simulation results confirm that the proposed GWO-based controller achieves superior performance in terms of transient response, disturbance rejection, and robustness, outperforming the other tested algorithms in all key performance metrics.

This paper is structured as follows: In Section 2, the structure and features of the PIDF controller are introduced. Section 3 presents the mathematical modeling of the engine speed control system and its implementation in Simulink. In Section 4, the design and application of the GWO for PIDF parameter tuning are discussed in detail. Section 5 provides a comprehensive comparison between the GWO-tuned controller and other metaheuristic algorithms, analyzing transient response, disturbance rejection, and frequency response. Finally, Section 6 concludes the study and outlines future research directions.

II. Overview of PIDF Controller

The PIDF controller is an enhanced form of the classical PID controller that incorporates a low-pass filter in the derivative term to reduce the effects of high-frequency noise. Its transfer function is expressed as:

$$PIDF(s) = K_P + \frac{K_I}{s} + \frac{Ns}{s+N}K_D \quad (1)$$

where, K_P, K_I, and K_D are the proportional, integral, and derivative gains, respectively, and N denotes the filter coefficient. This filtering action smooths the derivative response and prevents instability caused by rapid fluctuations or measurement noise, making the controller more suitable for practical applications. The structure of the PIDF controller used in this study is illustrated in Fig. 1.

III. Mathematical Modeling of Engine Speed Control System

This section presents the mathematical modeling and control structure of a four-cylinder spark ignition (SI) engine for engine speed regulation. The control strategy employs a PIDF controller to maintain the desired engine speed under varying operating conditions. The engine dynamics are modeled based on air intake, manifold pressure, and torque generation, and are implemented in MATLAB/Simulink.

A. Engine Dynamic Model

The engine's behavior is governed by a set of nonlinear differential equations that describe the interaction between throttle position, air mass flow, manifold pressure, and engine

torque. The following equations are derived from first principles and empirical modeling:

1) Throttle Airflow

The air mass flow rate entering the intake manifold, $\dot{m}_{ai}$, depends on throttle angle θ and the pressure ratio $\frac{P_m}{P_{amb}}$:

$$\dot{m}_{ai} = \begin{cases} f(\theta), if\ \frac{P_m}{P_{amb}} \leq 0.5 \\ f(\theta) \times g\left(\frac{P_m}{P_{amb}}\right), Otherwise \end{cases} \quad (2)$$

where P_m is the manifold pressure, P_{amb} is ambient pressure, and $f(\theta)$, $g\left(\frac{P_m}{P_{amb}}\right)$ are nonlinear functions derived from throttle flow characteristics.

2) Manifold Pressure Dynamics

$$\dot{P}_{\boldsymbol{m}} = \frac{RT}{V_m}(\dot{m}_{ai} - \dot{m}_{ao}) \quad (3)$$

where R is the gas constant, T is intake air temperature, V_m is the volume of the manifold, $\dot{m}_{ai}$ is the incoming air mass flow rate from the throttle, and $\dot{m}_{ao}$ is the outgoing air mass flow rate into the cylinders.

3) Intake Airflow in Cylinders

$$\dot{m}_{ao} = 0.366P_mN - 0.08979P_m^2 - 0.0337N^2 + 0.0001N^2P_m \quad (4)$$

where N is the engine speed in RPM, and P_m is manifold pressure in bar.

4) Engine Torque Generation

The engine torque T_{eng} is calculated as a nonlinear function of air mass m_a, air-fuel ratio $\frac{A}{F}$, spark timing σ, and engine speed:

$$T_{eng} = 181 + 3.379m_a - 36.21\left(\frac{A}{F}\right) + \cdots \quad (5)$$

5) Engine Speed Dynamics

$$\dot{N} = \frac{T_{eng} - T_{load}}{J} \quad (6)$$

where T_{load} is the load torque and J is the engine's rotational inertia.

B. Implement of PIDF in Engine Speed Control System

In general, PIDF controller enhances system robustness by incorporating a low-pass filter in the derivative path, minimizing sensitivity to noise.

Based on PIDF equation that express in section 2, In the time domain, the control signal θ is:

$$\theta = K_P e(t) + K_I \int_0^t e(\tau)\, d\tau + K_D \times Filtered\ (\frac{d}{dt}e(t)) \quad (7)$$

where $e(t) = N_{set}(t) - N(t)$ is the tracking error. The derivative is filtered using a first-order low-pass filter with cutoff determined by N.

C. Simulink Implementation and Response

The full engine model and PIDF controller are implemented in Simulink as illustrated in Fig. 2. The block diagram includes subsystems for engine dynamics, manifold pressure calculation, torque generation, and the PIDF controller block. The simulation tracks engine speed from 2000 to 3000 RPM under changing throttle commands.

Fig. 3 shows the time-domain response of the system, demonstrating that the PIDF controller achieves rapid convergence to the desired speed with minimal overshoot and steady-state error, validating its effectiveness in real-time control of engine dynamics.

IV. GWO-TUNED PIDF CONTROLLER DESIGN

A. Overview of Grey Wolf Optimizer

The GWO is a population-based metaheuristic optimization algorithm introduced by Mirjalili et al. [12]. It is inspired by the social hierarchy and hunting strategy of grey wolves in nature. In the algorithm, candidate solutions are represented as wolves, which are divided into four groups based on dominance: alpha (α), beta (β), delta (δ), and omega (ω). The alpha wolf represents the best solution found so far, while beta and delta help guide the search. The omega wolves follow the leading wolves and explore the search space accordingly.

In general, GWO algorithm is inspired by the natural hunting behavior of grey wolves, which involves a coordinated process of encircling the prey, collaboratively hunting it, and ultimately launching a final attack. This behavior is mathematically modeled to guide the search agents toward optimal solutions in a problem space.The positions of the wolves are updated iteratively using mathematical models that simulate the wolves' surrounding and attacking behaviors. GWO balances exploration and exploitation, making it highly effective for tuning controller parameters in nonlinear and complex systems.

In this paper, GWO is used to find the optimal PIDF controller parameters by minimizing the cost function (IAE), ensuring enhanced control accuracy and dynamic performance in engine speed regulation.

B. Objective Function Definition

The optimization goal is to minimize the integral of absolute error (IAE) over a simulation period of $t_f = 50s$ seconds, defined as:

$$IAE = \int_0^{t_f} |e(t)|dt \quad (8)$$

where $e(t) = r(t) - y(t)$ is the error between the reference speed $r(t)$ and the actual engine speed $y(t)$. This performance index penalizes both transient and steady-state errors, encouraging a fast and accurate response.

C. Parameter Boundaries

To ensure stability and practical implementation, the PIDF parameters are optimized within the constrained ranges given in Table I.

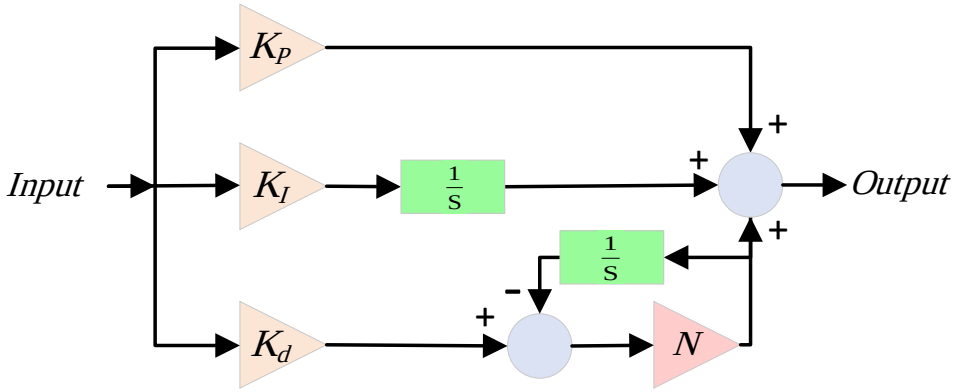

Fig. 1. General schematic of PIDF controller

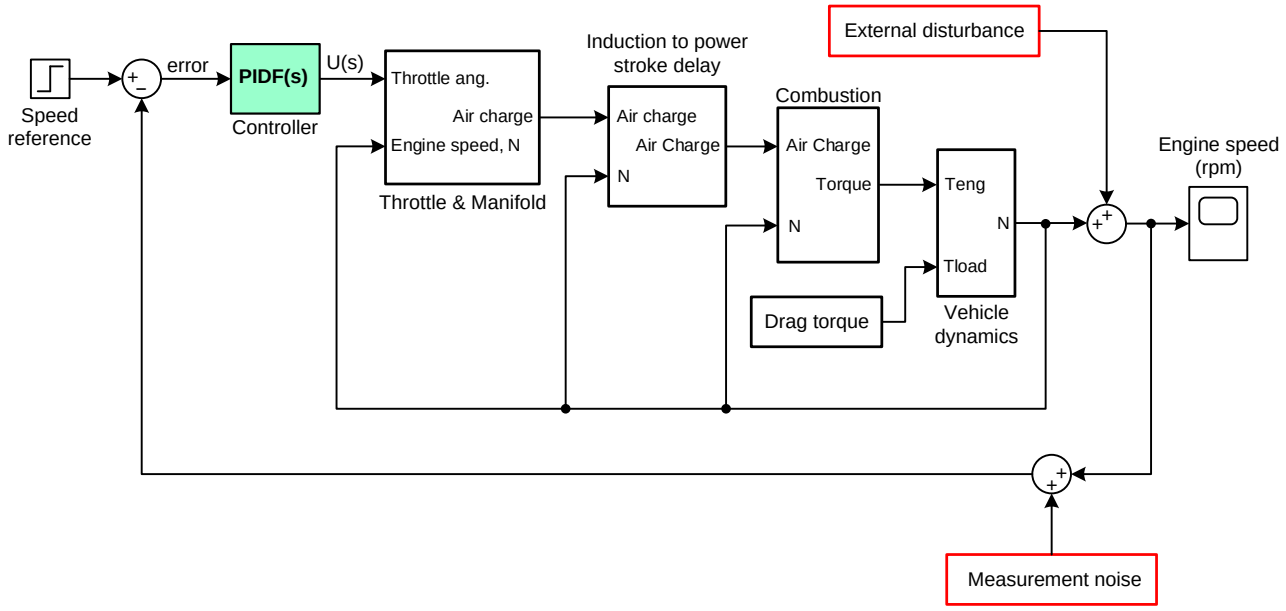

Fig. 2. Block diagram of PIDF controlled four-cylinder SI engine speed control system

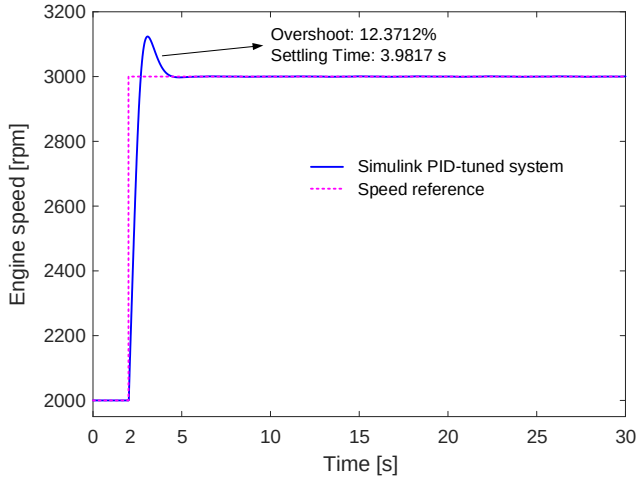

Fig. 3. Time response of Simulink PIDF-tuned system

TABLE I. BOUNDARIES FOR PIDF CONTROLLER PARAMETERS

Parameters	K_P	K_I	K_D	N
Lower Band	0.001	0.001	0.001	100
Upper Band	0.1	0.1	0.01	2000

These bounds were selected based on prior system knowledge and ensure the filter term is effective while keeping the gains within reasonable physical limits for the engine control unit.

D. System Implementation

The GWO algorithm is integrated with a closed-loop simulation model of the engine control system. Fig. 4 illustrates the structure of the control loop, where the PIDF controller processes the error signal and adjusts the throttle input accordingly. The engine's speed output is continuously monitored and compared with the reference to form the feedback signal.

The results of this tuning approach demonstrate that the GWO-tuned PIDF controller achieves a significant reduction in IAE compared to manually tuned or heuristically optimized controllers, with improved transient characteristics such as reduced overshoot and faster settling time.

V. COMPARATIVE SIMULATION RESULTS

This section presents the comparative simulation results of four metaheuristic optimization algorithms, GWO [12], CS [11], DE [10], and PSO [9] for tuning the parameters of a PIDF controller. The analysis includes statistical performance, transient response specifications, disturbance rejection, and frequency response characteristics.

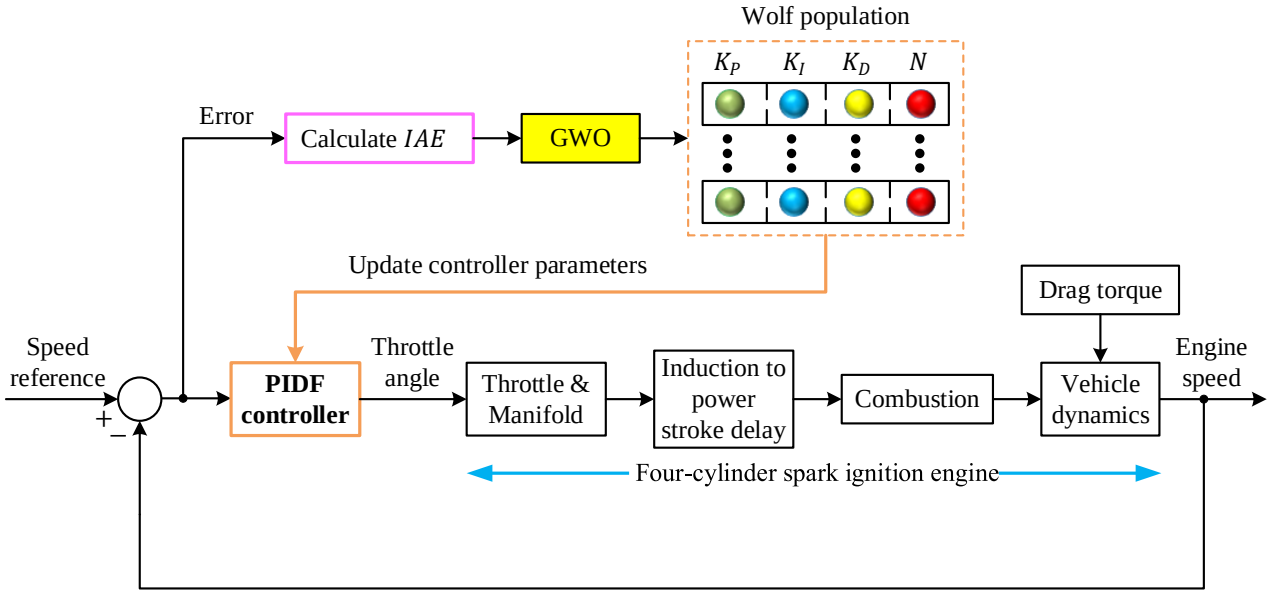

Fig. 4. Application of GWO to four-cylinder SI engine speed control system

A. *Experimental Setup*

All algorithms were executed over 25 independent runs under identical simulation conditions. The algorithmic parameters used for each method are summarized in Table II, where the population size and number of iterations were fixed to 30 and 50, respectively, across all methods. Additional tuning parameters such as mutation and recombination rates for DE, convergence constants for GWO, and inertia weights and acceleration coefficients for PSO were used as per their standard settings.

TABLE II. PARAMETER SETTINGS OF GWO, CS, DE AND PSO ALGORITHMS

Algorithm	Parameter	Value
GWO	Population size	30
	Total iteration number	50
	Convergence constant a	Decreases linearly from 2 to 0
CS	Population size	30
	Total iteration number	50
	Switching parameter p_a	0.25
DE	Population size	30
	Total iteration number	50
	Mutation rate	0.5
	Recombination rate	0.5
PSO	Population size	30
	Total iteration number	50
	Inertia weight w_{max} and w_{min}	[0.9, 0.6]
	Acceleration constants c_1 and c_2	[2, 2]

B. *Statistical Performance Evaluation*

Table III presents the statistical results of the best objective function values obtained in 25 independent runs. GWO demonstrated superior performance with the lowest mean (231.93), standard deviation (6.07), and minimum value (223.72), indicating both accuracy and consistency in finding optimal solutions.

Table IV demonstrates the Wilcoxon signed-rank test that confirmed the statistical significance of GWO's superiority over the other algorithms at a 5% significance threshold level.

TABLE III. STATISTICAL RESULTS OF THE BEST OBJECTIVE FUNCTION VALUES OBTAINED IN 25 INDEPENDENT RUNS

Algorithm	Mean	SD	Minimum	Maximum	Median
GWO	231.9312	6.0663	223.7207	251.9990	230.4099
CS	237.5224	7.4660	225.5810	249.8761	236.0028
DE	239.4535	7.2246	227.7941	252.7603	237.7943
PSO	238.1579	7.5903	227.6914	254.2174	236.7307

TABLE IV. WILCOXON SIGNED-RANK TEST BETWEEN PROPOSED OPTIMIZATION ALGORITHM AND OTHERS

GWO versus CS		GWO versus DE		GWO versus PSO	
p-value	Winner	p-value	Winner	p-value	Winner
0.0074	GWO	0.0013	GWO	0.0160	GWO

C. *Optimized PIDF Parameters*

The PIDF controller parameters tuned by each algorithm are shown in Table V. GWO achieved a well-balanced set of parameters that led to better control performance, as detailed in the next subsection.

TABLE V. OBTAINED PIDF PARAMETERS

Algorithm	K_P	K_I	K_D	N
GWO	0.097992	0.013252	0.0036819	217.17
CS	0.079164	0.013176	0.0033497	174.33
DE	0.095967	0.013339	0.0044356	1831.0
PSO	0.095805	0.013068	0.0033895	1739.9

Fig. 5 shows the convergence of PIDF parameters over iterations using the GWO, CS, DE and PSO algorithms. Initially, parameters fluctuate due to exploration, then gradually stabilize as the algorithm exploits the best regions. The smooth convergence indicates effective optimization. Final values ensure balanced and robust controller performance. Fig. 6 illustrates the convergence of the objective function over 50 iterations for the GWO, CS, DE and PSO algorithms. The objective value decreases rapidly in the early iterations, showing strong global search ability. It then gradually stabilizes, indicating convergence to an optimal solution. This smooth decline confirms the efficiency and reliability of the optimization process.

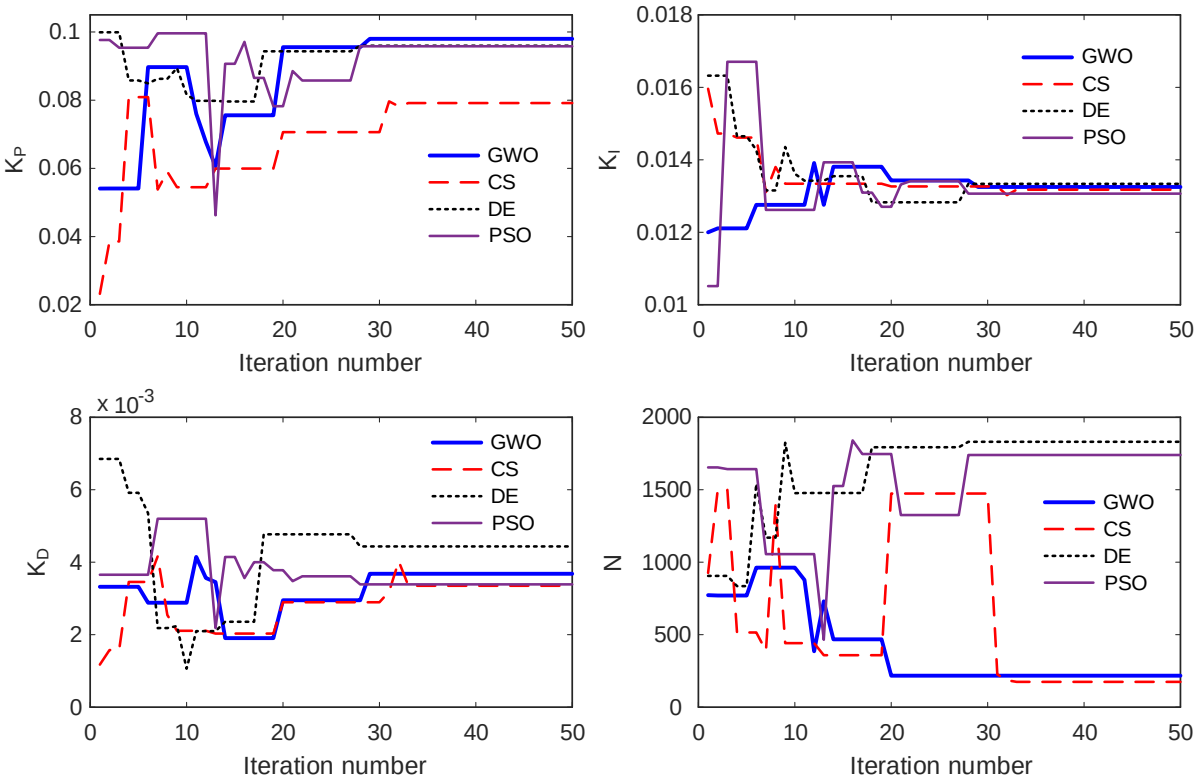

Fig. 5. Changes of PIDF controller parameters

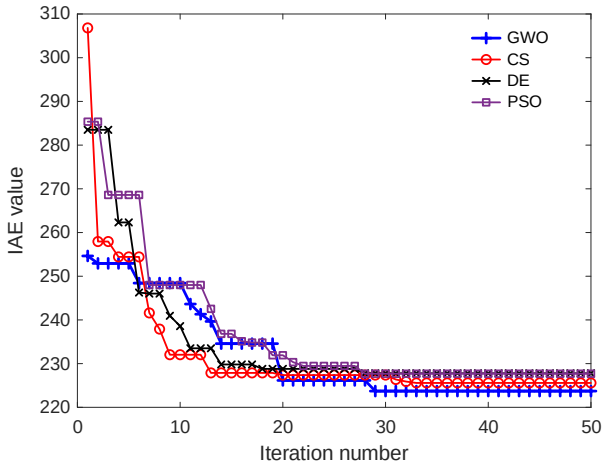

Fig. 6. Change of *IAE* objective function

D. Transient Response Analysis

The transient performance of the PIDF controllers optimized by GWO, CS, DE, and PSO algorithms is shown in Fig. 7 and Table VI. The GWO-tuned controller demonstrates a fast and smooth response with low overshoot and short settling time, reflecting its effective parameter tuning. To evaluate the performance quantitatively, five key transient specifications were analyzed: rise time, settling time, overshoot, peak time, and steady-state error.

The rise time was calculated based on the interval from 10% to 90% of the final value of the system output. The settling time was measured using a ±2% tolerance band around the final steady-state value. The steady-state error was computed at the final simulation time, t_f seconds. Under these definitions, the GWO method achieved the shortest rise time (0.3105 s), a fast settling time (2.4153 s), moderate overshoot (1.3765%), and a very low steady-state error of 1.8270×10^{-4} rpm. Although the DE algorithm produced the smallest overshoot (0.6124%), it exhibited a higher steady-state error compared to GWO. The CS and PSO algorithms also showed acceptable performance, but with slightly longer rise and settling times. Fig. 8 offers a magnified view of the time-domain responses, clearly emphasizing the faster convergence and reduced steady-state fluctuations achieved by the GWO-based controller.

TABLE VI. COMPARISONS OF NORMALIZED TRANSIENT RESPONSE SPECIFICATIONS

Algorithm	Rise time	Settling time	Overshoot	Peak time	Steady-state error
GWO	0.3105	2.4153	1.3765	2.4778	1.8270E−04
CS	0.3156	2.4268	0.9500	2.4932	4.0359E−05
DE	0.3142	2.4266	0.6124	2.4933	9.3574E−04
PSO	0.3113	2.4785	2.0069	2.4756	0.0010

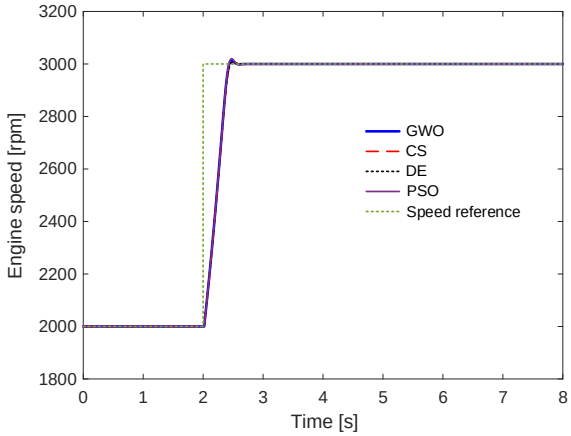

Fig. 7. Comparative time responses

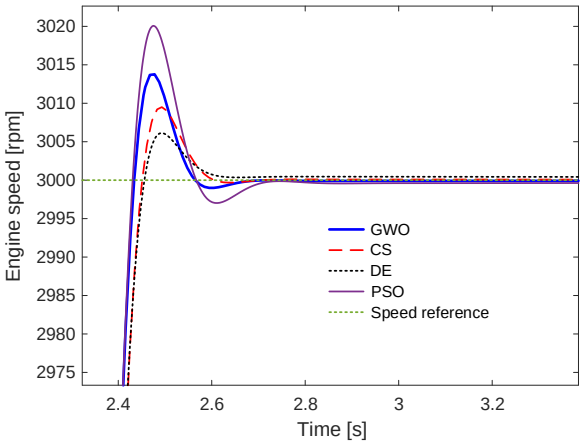

Fig. 8. Zoom of time responses

E. *Disturbance Rejection and Reference Tracking Performance*

To evaluate the robustness and real-world applicability of the GWO-based PIDF controller, the system was subjected to two types of external influences: a dynamic disturbance and measurement noise. As shown in Fig. 9, the external disturbance was defined in the Laplace domain as:

$$D(s) = -\frac{1740}{s^2 + 1.5s + 11.6} \tag{9}$$

and was applied starting from $t = 10s$, lasting throughout the remainder of the simulation. This disturbance mimics a real-life low-frequency perturbation that may affect the system's stability.

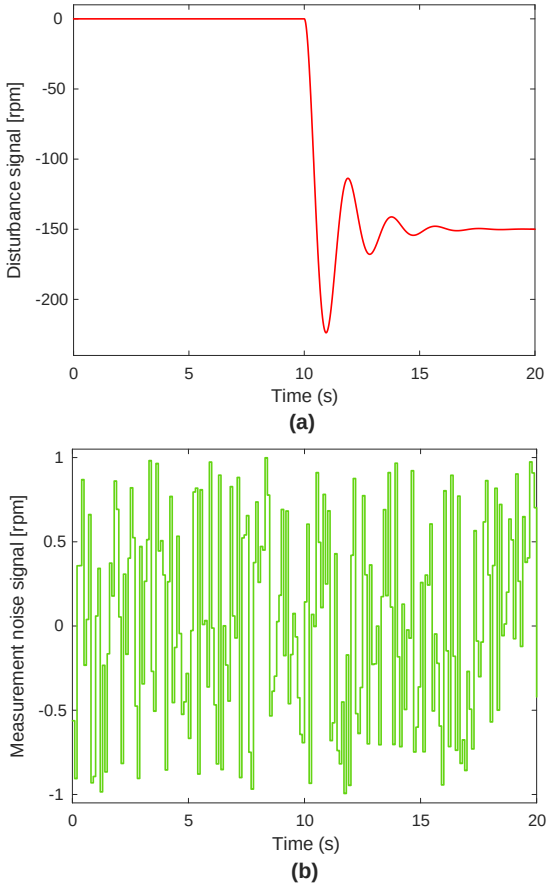

Fig. 9. Types of disturbances (a) external disturbance, (b) measurement noise

Simultaneously, measurement noise was introduced as a uniformly distributed random signal $\eta(t)$ within the range $[-1, 1]$, simulating sensor inaccuracies and electrical noise in the feedback signal. These conditions test the controller's ability to maintain performance under uncertainty and environmental noise.

Fig. 10 displays the system's time-domain response under these disturbance conditions. The GWO-optimized PIDF controller exhibits excellent disturbance rejection capability: despite the sudden onset of the disturbance and continuous noise, the system remains stable and maintains performance with only minimal deviation from the reference signal. This highlights the controller's robustness and effective damping behavior. In addition to disturbance rejection, the controller's ability to track varying reference signals was evaluated and is presented in Fig. 11. The results confirm that the GWO-based controller provides precise reference tracking, with minimal steady-state error and no noticeable lag or overshoot. This demonstrates that the controller is not only robust to external disturbances and noise but also capable of accurately following desired dynamic trajectories, making it suitable for real-world control applications.

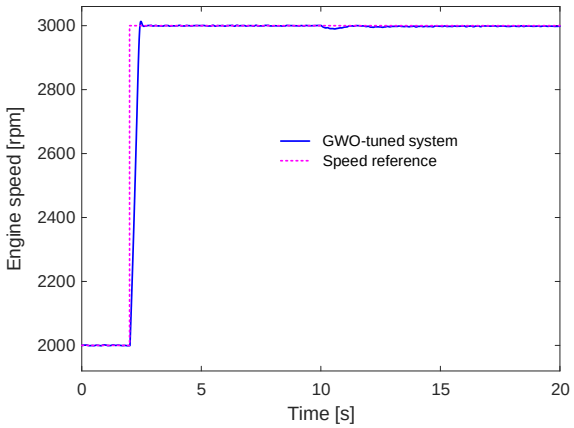

Fig. 10. Time response of GWO-based PIDF controlled system under disturbances

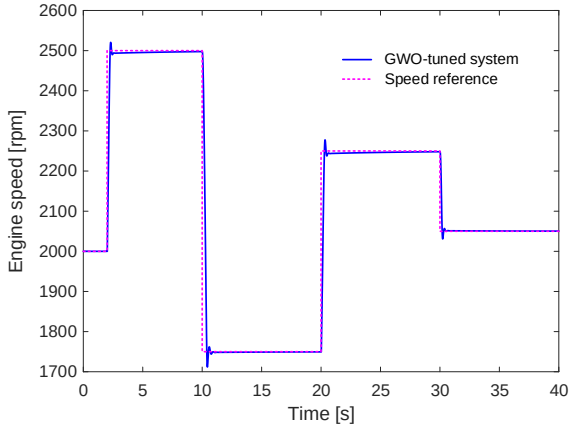

Fig. 11. Performance of GWO-based PIDF control in tracking reference input signal

F. *Frequency Response Analysis*

To assess the stability and robustness of the closed-loop system from a frequency-domain perspective, a Bode plot of the linearized open-loop transfer function of the GWO-based PIDF controlled system was analyzed, as shown in Fig. 12.

The frequency response reveals a gain margin of 12.8 dB at a frequency of 68.8 rad/s, and a phase margin of 34.6° at 22.3 rad/s. These values fall within the acceptable range for control systems, indicating that the system can tolerate moderate variations in gain and phase without becoming unstable.

A higher gain margin implies that the system can withstand larger increases in system gain before instability occurs, while a sufficient phase margin ensures good damping and transient behavior. The margins observed confirm that the designed controller not only performs well in time-domain simulations but also maintains robustness under frequency-domain criteria. Therefore, the Bode plot analysis supports the conclusion that the GWO-optimized PIDF controller guarantees closed-loop system stability with adequate robustness against uncertainties and unmodeled dynamics.

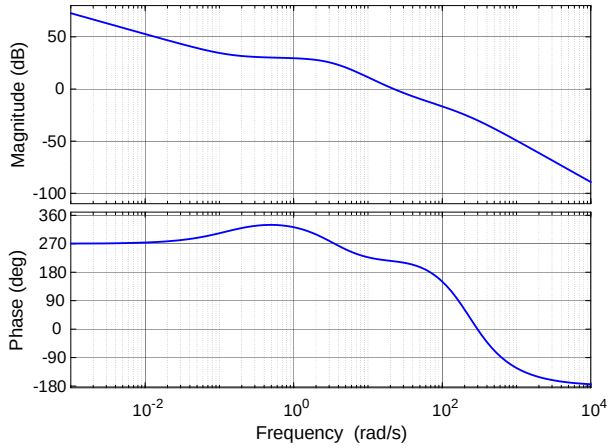

Fig. 12. Bode plot of open-loop GWO-based PID controlled system

VI. CONCLUSION

In this paper, a GWO-based PIDF controller tuning method was developed and applied to the speed control of a SI engine. By integrating the GWO algorithm with classical PID architecture, the proposed approach aimed to address, the inherent nonlinearities and disturbances present in internal combustion engine systems. Through comprehensive simulation experiments, the GWO-based controller demonstrated superior performance compared to traditional metaheuristic algorithms such as PSO, DE, and CS. The results showed improvements in transient response characteristics, reduced overshoot, enhanced disturbance rejection, and increased robustness.

Despite the promising results, the study has several limitations. The analysis was performed exclusively in a simulation environment, without real-time or hardware-in-the-loop (HIL) implementation. Additionally, the engine model assumes fixed parameters and does not account for long-term variations in engine wear or environmental conditions such as temperature or fuel quality. Moreover, while the tuning focused on PIDF parameters, other structural improvements for instance, fractional-order controllers or fuzzy hybrid systems were not considered.

From a practical and managerial perspective, the proposed GWO-based tuning method offers a low-cost, adaptive, and effective solution for real-time engine control systems. It can be integrated into embedded control units (ECUs) of vehicles to automatically adjust PIDF parameters under varying load and operational conditions, contributing to better fuel efficiency, smoother operation, and reduced emissions.

Future research may focus on extending the proposed framework to real-time hardware testing, applying the controller to different engine types, for instance, diesel or hybrid electric, and integrating more advanced control strategies, such as MPC or reinforcement learning-based methods. Additionally, hybrid optimization algorithms that combine the exploration strength of GWO with the exploitation ability of other techniques may further improve controller performance in dynamic environments.

REFERENCES

[1] M. Jabari, D. Izci, S. Ekinci, M. Bajaj, and I. Zaitsev, "Performance analysis of DC-DC Buck converter with innovative multi-stage PIDn (1+ PD) controller using GEO algorithm," *Scientific Reports*, vol. 14, no. 1, p. 25612, 2024.

[2] M. Jabari and A. Rad, "Optimization of speed control and reduction of torque ripple in switched reluctance motors using metaheuristic algorithms based PID and FOPID controllers at the edge," *Tsinghua Science and Technology*, vol. 30, no. 4, pp. 1526-1538, 2025.

[3] S. Ekinci, D. Izci, R. Ghandour, M. Salman, and C. Turkeri, "Aquila Optimizer-Based Filtered PID Controller Design for A Spark Ignition Engine Speed Control," in *2024 8th International Symposium on Innovative Approaches in Smart Technologies (ISAS)*, pp. 1-5, 2024.

[4] S. A. Alzakari, D. Izci, S. Ekinci, A. A. Alhussan, and F. A. Hashim, "A new control scheme for temperature adjustment of electric furnaces using a novel modified electric eel foraging optimizer," *AIMS Math*, vol. 9, no. 5, pp. 13410-13438, 2024.

[5] S. Ekinci, Ö. Can, M. Ş. Ayas, D. Izci, M. Salman, and M. Rashdan, "Automatic generation control of a hybrid PV-reheat thermal power system using RIME algorithm," *IEEE Access*, vol. 12, pp. 26919-26930, 2024.

[6] D. Izci, S. Ekinci, and A. G. Hussien, "An elite approach to re-design Aquila optimizer for efficient AFR system control," *Plos one*, vol. 18, no. 9, p. e0291788, 2023.

[7] M. Jabari, S. Ekinci, D. Izci, M. Bajaj, and I. Zaitsev, "Efficient DC motor speed control using a novel multi-stage FOPD (1+ PI) controller optimized by the Pelican optimization algorithm," *Scientific Reports*, vol. 14, no. 1, p. 22442, 2024.

[8] M. Jabari, M. A. Nasab, M. Zand, L. Tightiz, and S. Padmanaban, "Efficient parameter extraction in PV solar modules with the diligent crow search algorithm," *Discover Energy*, vol. 4, no. 1, p. 35, 2024.

[9] J. Kennedy and R. Eberhart, "Particle swarm optimization," in *Proceedings of ICNN'95-international conference on neural networks*, vol. 4, pp. 1942-1948, 1995.

[10] R. Storn and K. Price, "Differential evolution–a simple and efficient heuristic for global optimization over continuous spaces," *Journal of global optimization*, vol. 11, pp. 341-359, 1997.

[11] X.-S. Yang and S. Deb, "Cuckoo search: recent advances and applications," *Neural Computing and applications*, vol. 24, pp. 169-174, 2014.

[12] S. Mirjalili, S. M. Mirjalili, and A. Lewis, "Grey wolf optimizer," *Advances in engineering software*, vol. 69, pp. 46-61, 2014.

[13] P. Sharma, S. Raju, and R. Salgotra, "An evolutionary multi-algorithm based framework for the parametric estimation of proton exchange membrane fuel cell," *Knowledge-Based Systems*, vol. 283, p. 111134, 2024.

[14] L. Abualigah *et al.*, "Adaptive Gbest-Guided Atom Search Optimization for Designing Stable Digital IIR Filters," *Circuits, Systems, and Signal Processing*, pp. 1-23, 2025.

[15] M. Jabari *et al.*, "Parameter identification of PV solar cells and modules using bio dynamics grasshopper optimization algorithm," *IET Generation, Transmission & Distribution*, vol. 18, no. 21, pp. 3314-3338, 2024.

[16] A. Sahoo, S. Samantaray, and D. K. Ghose, "Multilayer perceptron and support vector machine trained with grey wolf optimiser for predicting floods in Barak river, India," *Journal of Earth System Science*, vol. 131, no. 2, p. 85, 2022.

[17] S. Yadav, P. Kumar, and A. Kumar, "Grey wolf optimization based optimal isolated microgrid with battery and pumped hydro as double storage to limit excess energy," *Journal of Energy Storage*, vol. 74, p. 109440, 2023.

[18] B. Nayak, A. Mohapatra, and K. B. Mohanty, "Parameter estimation of single diode PV module based on GWO algorithm," *Renewable Energy Focus*, vol. 30, pp. 1-12, 2019.

[19] S. Mohanty, B. Subudhi, and P. K. Ray, "A new MPPT design using grey wolf optimization technique for photovoltaic system under partial shading conditions," *IEEE Transactions on Sustainable Energy*, vol. 7, no. 1, pp. 181-188, 2015.

[20] D. Guha, P. K. Roy, and S. Banerjee, "Load frequency control of interconnected power system using grey wolf optimization," *Swarm and Evolutionary computation*, vol. 27, pp. 97-115, 2016.

[21] M. Rahmani, H. Komijani, and M. H. Rahman, "New sliding mode control of 2-DOF robot manipulator based on extended grey wolf optimizer," *International Journal of Control, Automation and Systems*, vol. 18, pp. 1572-1580, 2020.

[22] S. Chatterjee, V. Shaw, and R. Das, "Multi-stage intrusion detection system aided by grey wolf optimization algorithm," *Cluster Computing*, vol. 27, no. 3, pp. 3819-3836, 2024.

[23] Q. Al-Tashi, H. Md Rais, S. J. Abdulkadir, S. Mirjalili, and H. Alhussian, "A review of grey wolf optimizer-based feature selection methods for classification," *Evolutionary machine learning techniques: algorithms and applications*, pp. 273-286, 2020.

[24] D. K. Geleta, M. S. Manshahia, P. Vasant, and A. Banik, "Grey wolf optimizer for optimal sizing of hybrid wind and solar renewable energy system," *Computational intelligence*, vol. 38, no. 3, pp. 1133-1162, 2022.

[25] J. Czarnigowski, "A neural network model-based observer for idle speed control of ignition in SI engine," *Engineering Applications of Artificial Intelligence*, vol. 23, no. 1, pp. 1-7, 2010.

[26] Y. Yildiz, A. M. Annaswamy, D. Yanakiev, and I. Kolmanovsky, "Spark-ignition-engine idle speed control: An adaptive control approach," *IEEE Transactions on Control Systems Technology*, vol. 19, no. 5, pp. 990-1002, 2010.

[27] J. Duarte, J. Garcia, J. Jimenez, M. E. Sanjuan, A. Bula, and J. Gonzalez, "Auto-ignition control in spark-ignition engines using internal model control structure," *Journal of Energy Resources Technology*, vol. 139, no. 2, p. 022201, 2017.

[28] Q. Zhu, R. Prucka, M. Prucka, and H. Dourra, "A nonlinear model predictive control strategy with a disturbance observer for spark ignition engines with external EGR," *SAE International Journal of Commercial Vehicles*, vol. 10, no. 2017-01-0608, pp. 360-372, 2017.

[29] W. Wang, E. Chirwa, E. Zhou, K. Holmes, and C. Nwagboso, "Fuzzy ignition timing control for a spark ignition engine," *Proceedings of the Institution of Mechanical Engineers, Part D: Journal of Automobile Engineering*, vol. 214, no. 3, pp. 297-306, 2000.

[30] R. K. Sahu and D. K. Srivastava. *Model Based Calibration of a Multi Cylinder Spark Ignition Engine for Idle Speed Control Using PID Control Strategy*. SAE Technical Paper, 2023.